scientific reports

Check for updates

OPEN

# Daidzein alleviates skin fibrosis by suppressing TGF-β1 signaling pathway via targeting PKM2

Xiaowei Guo[1,6], Wenqi Li[1,6], Wei Ma[3,6], Yuming Liu[1], Zhigang Liu[1], Ran Jiao[1], Zhongyi Yang[1], Tiantian Zhang[1], Hongliang Wu[5], Xiaoyu Ai[1,2], Xiaoting Gu[1,2], Wendi Wang[4], Honggang Zhou[1,2]✉, Xiaohe Li[1,2]✉ & Cheng Yang[1,2]✉

**Skin fibrosis including keloids, which are characterized including excessive deposition, abnormal proliferation, aggressiveness, and migration of the extracellular matrix of dermal fibroblasts. TGF-β signaling is a classical pro-fibrotic pathway, and it plays a crucial part in the occurrence and progression of skin fibrosis. Daidzein (Dai), an isoflavone compound, has been proved to possess anti-fibrosis effect by TGF-β signaling in various inflammatory and fibrotic diseases. However, little is known about Dai on skin fibrosis. Therefore, we further explored the potential effects and mechanisms of daidzein on skin fibrosis. As expected, Dai suppressed proliferation, migration and activation mouse primary dermal fibroblasts and keloid fibroblasts. Meanwhile, Dai also ameliorated bleomycin-induced skin fibrosis and reduced fibrotic markers of keloid tissues. In addition, Dai could target PKM2 to inhibit TGF-β1/Smad signaling in skin fibrosis. Overall, our research demonstrated that Dai might become a potential therapeutic candidate drug for skin fibrosis.**

**Keywords** Skin fibrosis, Keloid, TGF-β signaling, Daidzein, PKM2

**Abbreviations**

| | |
|---|---|
| BLM | Bleomycin |
| CTL | Control |
| Col-1 | Collagen-I |
| Dai | Daidzein |
| DF | primary dermal fibroblast |
| Fn | Fibronectin |
| KF | Keloid fibroblast |
| PKM2 | pyruvate kinase M2 |

Fibrogenesis is a widespread and general process, which is associated with tissue healing[1]. Fibrosis is manifested by the over proliferation of fibroblasts and over-accumulation of the extracellular matrix. Among them, skin fibrosis is related to abnormal repair after deep dermal injury, which often occurs in the process of repairing injuries such as surgery and burns[2]. Keloids is a classical type of skin fibrosis, which is often persistently growing and rarely resolve spontaneously[3], and some patients are accompanied by itching, pain, and limited joint mobility, which seriously affects the quality of their life[4]. Its pathogenesis is unknown, and keloid fibroblasts are thought to be the main effector cells in keloid formation, which are associated with excessive deposition, abnormal proliferation, aggressiveness, and migration of the extracellular matrix[5].

TGF-β1 has been proven to be the major regulator of the progress of fibrosis, and deregulated the fibroblasts activation and collagen synthesis by Smad signaling and non-Smad pathways[6,7]. In addition, it could inhibit the activity of matrix metalloproteinases[8]. Current treatment methods mainly focus on surgical resection and

[1]State Key Laboratory of Medicinal Chemical Biology, College of Pharmacy, College of Life Sciences, Nankai University, Tianjin 300353, China. [2]Tianjin Key Laboratory of Molecular Drug Research, Tianjin International Joint Academy of Biomedicine, Tianjin 300457, China. [3]Department of Burn and Plastic Surgery, Tianjin Fourth Hospital, Tianjin 300222, China. [4]Department of Plastic and Burn Surgery, Tianjin First Central Hospital, No. 24 Kangfu Road, Nankai District, Tianjin 300192, China. [5]Department of Anesthesiology, National Clinical Research Center for Cancer/Cancer Hospital, National Cancer Center, Chinese Academy of Medical Sciences and Peking Union Medical College, No. 17 Nanli, Panjiayuan, Chaoyang District, Beijing, China. [6]These authors contributed equally: Xiaowei Guo, Wenqi Li and Wei Ma. ✉email: honggang.zhou@nankai.edu.cn; lixiaohe908@163.com; cheng.yang@nankai.edu.cn

intralesional steroid injection[9], but the prognosis is poor and it is easy to recur, so it is significant for us to find a drug that can effectively improve and treat keloid disease.

Daidzein (7,4-dihydroxyisoflavone) belongs to the phytoestrogen compound, mainly appeared in soy foods and soybeans, and is an isoflavone compound[10]. Experiments have shown that soy flavonoids had positive effects on cardiovascular disease, such as heart failure[11], with antioxidant, anti-inflammatory and anti-apoptotic abilities. Previous studies also have indicated Dai alleviated cardiac fibroblast activation by TGF-β1 stimulation[12] and significant therapeutic impacts on BLM-induced pulmonary fibrosis[13]. However, little is known on Dai about skin fibrosis. Therefore, the aim of the paper was to explore the antifibrotic effects and potential mechanisms of Dai on skin fibrosis.

## Materials and methods

### Human keloid tissue samples

Keloid tissues were obtained from patients of Tianjin Fourth Hospital, Nankai University. All participants in our research provided informed consent before study, and all methods were performed in accordance with relevant guidelines and regulations. The study was approved by the Ethics Committee of Nankai University (approval No. NKUIRB2020064).

### Isolation and culture of keloid fibroblasts

Keloid fibroblasts (KFs) were isolated based on previous article above[14].

### Isolation and culture of primary dermal fibroblasts

Primary dermal fibroblasts (DFs) from newborn mice were isolated based on previous methods[15].

### CCK-8 assay

The amount of $10^3$ per well were cultured in 96-well plates, cultured with diverse doses of Dai (0, 12.5 and 25 μM), and then added CCK-8 reagent (Dojindo, CK04) at different days with at 37℃ for 4 h. The OD450nm absorbance was then recorded.

### EdU incorporation assay

Cell proliferation was observed with the BeyoClickTM EdU-555 Imaging Kit (Beyotime Biotechnology, China). After 48 h treatment with different concentrations of Dai, an equal EDU was added for 2 h. Then, cells were fixed in 4% polymerization paraformaldehyde (PFA), and incubated with a Click Additive Solution for 30 min. Use LSM 800 (Zeiss, Germany) to focus on the microscope to detect immunofluorescence signals.

### Wound-healing assay

Cells were performed to make a straight scratch with a sterile 200 μL tip. Cells were pretreated with Dai ahead for 1 h, then added TGF-β1 (10 ng/mL) or not for next 24 h. The scratch was observed from three random fields.

### Transwell assays

Transwell Chambers (Corning, USA) was used to investigate the anti-migration effect of Dai. The $5\times10^4$ fibroblasts were suspended with serum-free DMEM and then spread in the transwell chamber. 15% FBS DMEM medium was added to the petri dish below the chamber. After the cells were incubated with Dai of different concentrations for 48 h, the cells were fixed with 4% paraformaldehyde, stained with crystal violet, and the number of migrating cells on the back of the cells was counted under the microscope.

### Explant culture of human keloid tissues

The isolated patient keloid tissues were cut into small pieces and cultured in a cell culture dish with DMEM supplemented with 20% FBS, taking care that the page of the culture medium did not completely cover the tissue. After the tissue stick to the bottom, different concentrations of Dai were added to the medium. On days 0 and 9, representative photographs of the migration of KFs from the edge of the tissue were taken.

### Quantitative real-time PCR (qRT-PCR)

UNICON® qPCR SYBR Green Master Mix (Yeasen Biotech, China) was used for qRT-PCR. GAPDH or β-Actin were served as endogenous control genes. Gene expression was calculated by $2^{-\Delta\Delta CT}$ method. The sequences of primer were in Table 1.

### Western blot analysis

Total proteins were collected from cells or tissues using RIPA buffer. The protein concentration was determined using BCA Protein Assay Kit (Beyotime, China). Equal proteins were analyzed by SDS-PAGE. Then, we used ECL system (Affinity, USA) to conduct the results. GAPDH and β-Tubulin were served as loading controls. Finally, the results were quantified by Image J for independent experiments. The antibodies were in Table 2.

### Immunofluorescence staining

Cells were incubated with rabbit anti-α-SMA (Affinity, AF1032, USA), anti-Collagen I (CST, 72026, USA) or anti-Phospho-Smad3 (CST, 9520, USA) overnight at 4 °C, followed by FITC-conjugated secondary antibody (Jackson, 115-095-003/111-025-003) and DAPI (Solarbio, S2110). Use LSM 800 (Zeiss, Germany) to focus on the microscope to detect immunofluorescence signals. Finally, the results were quantified by Image J for independent experiments.

| Gene | Forward sequence (5'-3') | Reverse sequence (3' -5') |
|---|---|---|
| α-SMA (Mouse) | GCTGGTGATGATGCTCCCA | GCCCATTCCAACCATTACTCC |
| Col-1α (Mouse) | CCAAGAAGACATCCCTGAAGTCA | TGCACGTCATCGCACACA |
| Fn (Mouse) | AAGGATGGAGTGATAGCAACCC | TCTGCTTGAAATCTGGTGTGC |
| GAPDH (Mouse) | TGGATTTGGACGCATTGGTC | TTTGCACTGGTACGTGTTGAT |
| MMP-1 (Mouse) | GTCACTCCCTTGGGCTCAC | TGCTGCCTTTGAAATAGCGGAC |
| MMP-2 (Mouse) | TGGCACCACCGAGGACTATGAC | ACACCACACCTTGCCATCGTTG |
| MMP-13 (Mouse) | ATGATGAAACCTGGACAAGCAG | CTGGGTCACACTTCTCTGGT |
| TIMP-1 (Mouse) | ACAAGTCCCAGAACCGCAG | TGGATTCCGTGGCAGGCA |
| α-SMA (Human) | TGGGTGAACTCCATCGCTGTA | GTCGAATGCAACAAGGAAGCC |
| Col-1α (Human) | AAGCCGGAGGACAACCTTTTA | GCGAAGAGAATGACCAGATCC |
| β-actin (Human) | AGGCCAACCGTGAAAAGATG | AGAGCATAGCCCTCGTAGATGG |
| MMP-1 (Human) | GGAGCTGTAGATGTCCTTGGGGT | GCCACAACTGCCAAATGGGCTT |
| MMP-2 (Human) | CAAAAACAAGAAGACATACATCTT | GCTTCCAAACTTCACGCTC |
| MMP-13 (Human) | AGTGGTGGTGATGAAGATGATTTG | CATTTCTCGGAGCCTCTCAGTC |
| TIMP-1 (Human) | TGACATCCGGTTCGTCTACA | TGCAGTTTTCCAGCAATGAG |

**Table 1**. Primers for QRT-PCR.

| Antibody | Company | No |
|---|---|---|
| α-SMA | Affinity | AF1032 |
| Col-1 | Cell signaling technology | 72,026 |
| Fn | Proteintech | 15,613-AP |
| Phospho-Smad2 | Cell signaling technology | 18,338 |
| Smad2 | Cell signaling technology | 5339 |
| Phospho-Smad3 | Cell signaling technology | 9520 |
| Smad3 | Cell signaling technology | 9523 |
| PKM2 | Affinity | AF5234 |
| GAPDH | Affinity | AF7021 |
| β-Tubulin | Affinity | AF7011 |

**Table 2**. The antibodies for Western blot.

## Animals

6–8 weeks male C57BL/6 mice and 10 weeks female nude BALB/c mice were bought from Beijing Vital River Laboratory Animal Technology (Beijing, China). The animal study was approved by the Institutional Animal Care and Use Committee (IACUC) of Nankai University (No. SYXK 2019-0001) and all methods were performed in accordance with relevant guidelines and regulations.

## Bleomycin-induced skin fibrosis model

This model was established by continuous daily injection of BLM sulfate (100 μL, 700 μg/mL in saline) on the back skin for 3 weeks. Mice were randomly divided into five groups: NaCl group, BLM group, BLM + Dai-12.5μM group, BLM + Dai-25μM group, BLM + Dai-50μM group. In NaCl group, mice were daily administrated with equal vehicle (sterile saline plus 1% DMSO). In BLM group, mice were daily injected with 100 μL BLM sulfate. In Dai treatment groups, mice were injected with 100 μL BLM as well as Dai (12.5, 25, 50 μM). Mice were anesthetized by Lidocaine hydrochloride (Sangon Biotech, China). This model was used for curative treatment of Dai on skin fibrosis.

## Keloid xenograft mouse model

This model was established according to previous protocol[16]. After surgery for two weeks, mice were injected with vehicle (phosphate buffer solution) or Dai (12.5, 25, 50 μM) three times a week for two weeks. This model was used for curative treatment of Dai on skin fibrosis.

## Histological examination

Mouse skin tissues and keloid tissues were fixed in 10% formalin for 24 h, and then embedded in paraffin to prepare 5 μm tissue sections. After dewaxing, tissue sections were stained with Masson trichrome, Picrosirius red (Solarbio, China), and hematoxylin and eosin (H&E). Random photographs were taken using an upright transmission fluorescence microscope (Olympus, Japan). Finally, the results were quantified by Image J for independent experiments.

### Hydroxyproline content determination
Mouse skin samples were dried and hydrolyzed in hydrochloric acid, then hydroxyproline (HYP) content was measured using a HYP detection kit (Solarbio, China) according to kit instructions.

### Immunohistochemistry staining
Skin tissues section (5 μm) were dewaxing and added with antibodies (α-SMA, Col-1, Phospho-Smad3 and PKM2), and images were captured with a fluorescence microscope (Olympus). Finally, the results were quantified by Image J for independent experiments.

### Drug affinity responsive target stability (DARTS)
Following cell culture, gather the cells using M-PER lysis buffer (adding protease and phosphatase inhibitors), centrifuge at room temperature for 10 min (18,000 ×g), the supernatant was transferred and measured the protein concentration; 4–6 μg/μl may be the ideal range for DARTS; After dividing the lysate into seven tubes and bringing them back to room temperature, add three ¼l of the medication to one tube and three ul of solvent to the remaining six tubes. Incubate for one hour at room temperature. To every part, 2 μl of a 1:200 enzyme solution was added, thoroughly mixed, and allowed to incubate for 30 min at room temperature, in addition to the control group.

### In-gel digestion for mass spectrometric characterization of proteins
First, the target protein band on the electrophoresis gel should be cut off, then the strip should be cleaned and decolorized, the cut strip should be washed with water and added with decolorization solution for decolorization, and then treated with ammonium bicarbonate and acetonitrile to completely fade the color of the strip and be placed to dry naturally at 37 °C for 4–6 h; Finally, the protease solution was added to the dried colloids to make the colloids completely bubble and the proteins in the colloids were fully enzymatically hydrolyzed. The encoded peptides were extracted from TFA and acetonitrile solutions and lyophilized, so that protein peptide samples that could be analyzed by mass spectrometry were obtained.

### Molecular Docking
The docking target is PKM2 and the PDB ID of the crystal structure used is 6V76. The docking software is AutoDockTools 4.2.6 software.

### Cellular thermal shift assay (CETSA)
CETSA was used to show the stability between target protein and compound. Dai (50 μM) was added to 80% confluent DFs cells in 100 mm dishes. And then cells were collected and resuspended in RIPA lysate. Divide the cell suspension into 10 RNA-free tubes, and placed at different temperatures (50, 53, 56, 59, 62, 65, 68, 71, 74, and 77 ℃) for 5 min. The supernatant was determined and analyzed by SDS-PAGE.

### Cell transfection
A slience RNA against PKM2 (siRNA-PKM2: 5'-CAUCUACCACUUGCAAUUATT-3') and a negative control siRNA (siRNA-NC: 5'-UAAUUGCAAGUGGUAGAUGTT-3') were measured to knock down PKM2. Lipofectamine RNAi MAX Transfection Reagent (Invitrogen, USA) was used in DFs for 24 h. Then collected cells and extracted protein for Western blot experiments.

### Statistical analysis
Data were analyzed by Prism 8.3.0 with results shown as the Mean ± SD. Group comparisons were performed using one-way ANOVA by Tukey's post hoc test for multiple comparison tests. $P < 0.05$ was considered to indicate statistical significance. We confirmed that all the study was reported in accordance with ARRIVE guidelines.

## Results
### Dai alleviates TGF-β1-induced mouse primary skin fibroblasts proliferation and migration
To begin with, we investigated the toxic level of Dai in DFs. The CCK-8 results showed that the IC50 of Dai was 331.8 μM (Fig. 1A). Referring to previous studies[12], we chose three concentrations (12.5, 25, and 50 μM) in our research. Then, we explored Dai on cell proliferation and migration of TGF-β1-induced DFs. As expected, CCK-8 and EdU results showed that cell proliferation level was increased significantly under TGF-β1 stimulation, while decreased in a dose-dependent manner after treatment with three doses of Dai (Fig. 1B, C). As for cell migration, wound-healing results suggested a significant inhibitory effect of Dai in TGF-β1-activated DFs (Fig. 1D). Meanwhile, transwell analysis was also observed the similar result (Fig. 1E). Besides, Dai also inhibited the ratio of matrix metalloproteinases to matrix metalloproteinase inhibitors (Fig. 1F). Taken together, these data demonstrated that Dai alleviated TGF-β1-induced DFs proliferation and migration in vitro.

### Dai suppresses keloid fibroblasts proliferation and migration
To verify Dai on abnormally proliferating fibroblasts in keloids, we further detected that the IC50 of Dai on KFs was 231.4 μM (Fig. 2A). Interestingly, cell proliferation was dose-dependent inhibited over a period of 9 days (Fig. 2B). The same results were verified by EdU experiments (Fig. 2C). Meanwhile, Dai was able to significantly suppress the migration of KFs (Fig. 2D, E). Besides, ex vivo keloid explant culture model was used to further investigate Dai on KFs migration. Expectedly, keloid explant model showed the similar conclusion (Fig. 2F). In addition, Dai also inhibited the ratio of matrix metalloproteinases to matrix metalloproteinase inhibitors (Fig. 2G). Taken together, these data suggested that Dai suppressed KFs proliferation and migration in vitro.

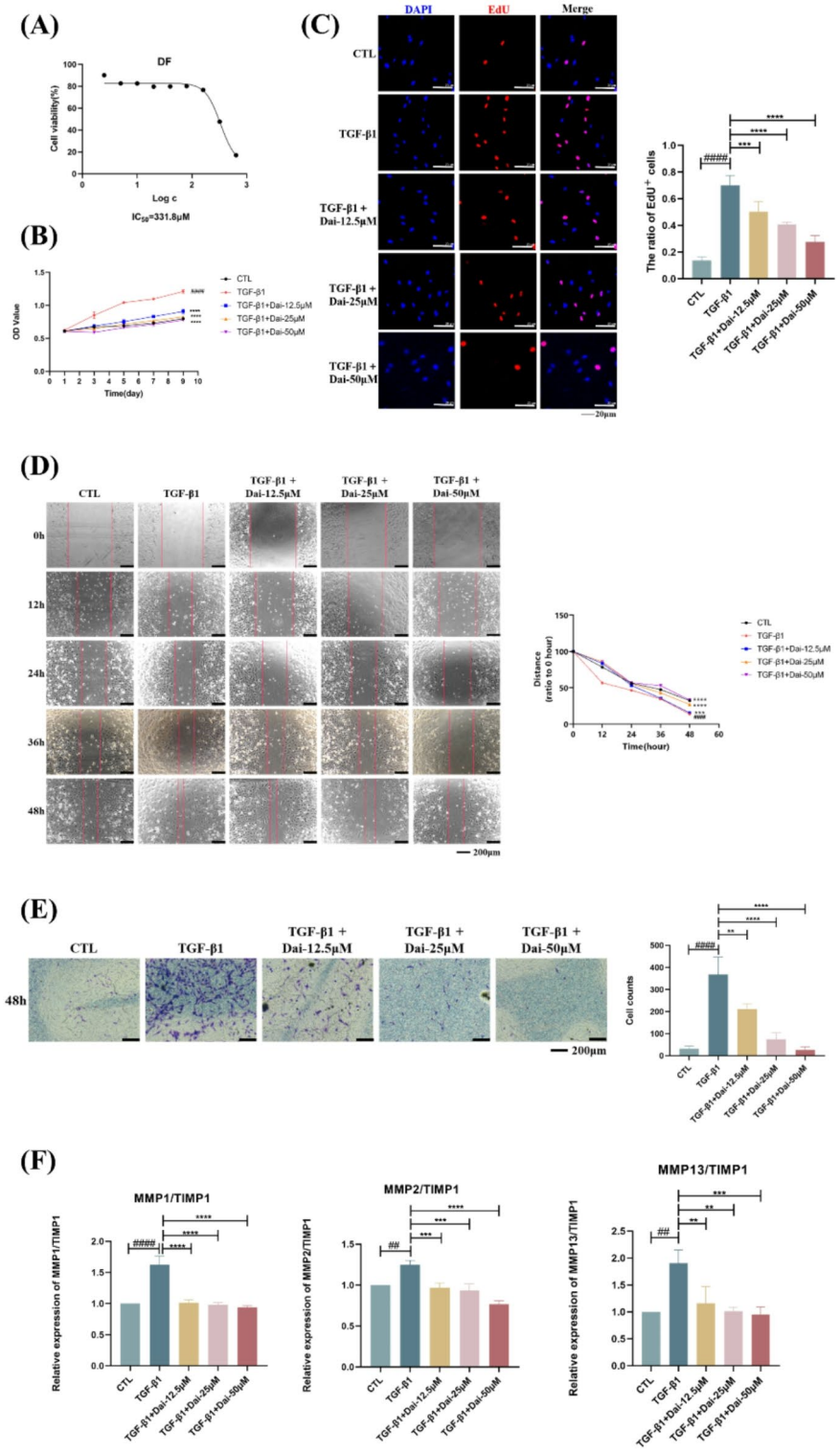


**Fig. 1**. Daidzein inhibits TGF-β1-induced proliferation and migration of mouse primary dermal fibroblasts. (**A**) CCK-8 analysis cell toxicity of Dai in DFs ($n = 3$); (**B**) CCK-8 analysis cell viability of Dai in DFs ($n = 3$); (**C**) Representative images and quantitative results of EdU incorporation assay in DFs ($n = 5$) (40×, scale bar = 20 μm); (**D**) Representative images and quantitative analysis of wound healing assay in DFs ($n = 5$) (20×, scale bar = 200 μm); (**E**) Representative images and quantitative results of migration in DFs ($n = 5$) (20×, scale bar = 200 μm); (**F**) The mRNA levels of MMP-1, MMP-2 and MMP-13 in DFs ($n = 5$). The data are shown as Mean ± SD, one-way ANOVA with Tukey's post-hoc multiple comparison tests. ####, $p < 0.0001$ vs. CTL; **, $p < 0.01$, ***, $p < 0.001$, ****, $p < 0.0001$ vs. TGF-β1. CTL, Control; Dai, Daidzein; DFs, Mouse primary dermal fibroblasts.

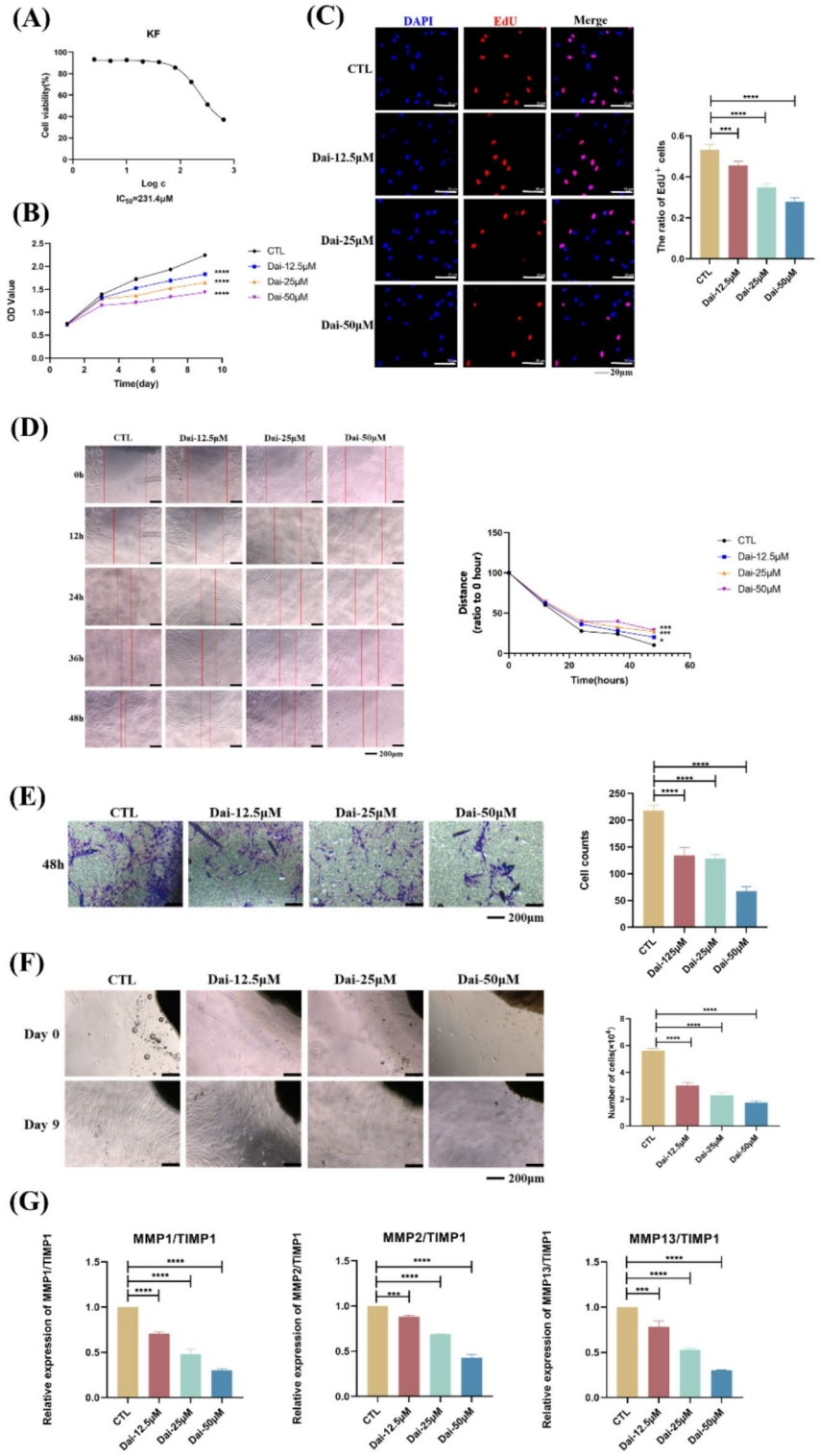


**Fig. 2**. Daidzein suppresses the proliferation, migration of keloid fibroblasts. (**A**) CCK-8 analysis cell toxicity of Dai in KFs ($n = 3$); (**B**) CCK-8 analysis cell viability of Dai in KFs ($n = 3$); (**C**) representative images and quantitative results of EdU incorporation assay in PSFs ($n = 5$) (40×, scale bar = 20 μm); (**D**) representative images and quantitative analysis of wound healing assay in KFs ($n = 5$) (20×, scale bar = 200 μm); (**E**) representative images and quantitative results of migration in KFs ($n = 5$) (20×, scale bar = 200 μm); (**F**) representative images of tissue explants of KFs ($n = 5$) (40×, scale bar = 200 μm). The cell numbers that migrated out of the tissue explants were quantified at day 9; (**G**) The mRNA levels of MMP-1, MMP-2 and MMP-13 in KFs ($n = 5$). The data are shown as mean ± SD, one-way ANOVA with Tukey's post-hoc multiple comparison tests. ***, $p < 0.001$, ****, $p < 0.0001$ vs. CTL. CTL, Control; Dai, Daidzein; KFs, Keloid fibroblasts.

### Dai prevents mouse primary dermal fibroblasts activation by TGF-β1-Smad2/3 signaling

As mentioned above, Dai alleviated TGF-β1-induced DFs proliferation and migration. Then, we further investigated the expression of fibrotic genes in TGF-β1-induced DFs. Consistently, Dai dose-dependent reduced TGF-β1-induced the expression of α-SMA, Collagen-I (CoL-1α), and Fibronectin (Fn) both in mRNA and protein level (Fig. 3A, B). As for mechanism study, results showed that the phosphorylation level of Smad2 and Smad3 were apparently increased by TGF-β1, while decreased under treatment of Dai (Fig. 3C). We also confirmed that Dai also reduced TGF-β-non-Smad signal pathway (Figure S1). Similarly, immunofluorescence analysis indicated the same results (Fig. 3D–F). Taken together, these data demonstrated that Dai prevented DFs activation by TGF-β-Smad2/3 signaling in vitro.

### Dai reduces keloid fibroblasts activation by TGF-β-Smad2/3 signaling

Next, we detected whether Dai had a direct impact on KFs. Consistently, Dai dose-dependent reduced the expression of α-SMA, Collagen-I (CoL-1α), and Fibronectin (Fn) both in mRNA and protein level (Fig. 4A, B). As for mechanism study, results showed that the phosphorylation level of Smad2 and Smad3 were decreased under treatment of Dai (Fig. 4C). We also confirmed that Dai also attenuated TGF-β-non-Smad signal pathway (Figure S2). Similarly, immunofluorescence analysis proved the same results (Fig. 4D–F). Taken together, these data suggested that Dai reduced KFs activation in vitro.

### Dai ameliorates BLM-induced skin fibrosis

To determine whether Dai had an effect in vivo, on, we soon investigated Dai on BLM-induced skin fibrosis in mice. Interestingly, Dai reduced dermal thickness and collagen stimulation in BLM-induced mice (Fig. 5A–C). Besides, Dai also decreased hydroxyproline content, which reflected on the level of skin fibrosis (Fig. 5D). Meanwhile, Dai suppressed α-SMA, Col-1α, Fn, MMP-1/TIMP-1, MMP-2/TIMP-1 and MMP-13/TIMP-1 both in mRNA and protein level (Fig. 5E, F). As for mechanism study, results showed that the phosphorylated Smad2 and Smad3 were apparently increased by BLM, while decreased under treatment of Dai (Fig. 5G). Similarly, immunohistochemistry analysis demonstrated the same results (Fig. 5H and J). Taken together, these data indicated that Dai ameliorated BLM-induced skin fibrosis by TGF-β-Smad2/3 signal in vivo.

### Dai ameliorates xenografted keloid tissue fibrogenic activation

Besides, we further used a nude mouse model of keloid xenografts, which was to simulate the internal environment of keloid patients. Similarly, results showed that the tissue weight treated with Dai was lighter than that of the control group (Fig. 6A). Meanwhile, Dai suppressed the collagen deposition (Fig. 6B). As for fibrotic markers, Dai inhibited the expression of α-SMA, Col-1α, Fn, MMP-1/TIMP-1, MMP-2/TIMP-1 and MMP-13/TIMP-1 both in mRNA and protein level (Fig. 6C, D). In addition, immunohistochemistry analysis demonstrated the same results (Fig. 6E, F). Taken together, these data indicated that Dai ameliorated the regression of xenograft keloid in vivo.

### Dai binds to PKM2 to inhibit mouse primary dermal fibroblasts activation

Since PKM2 was reported to be involved in multiple fibrotic diseases and promoted fibroblasts proliferation, migration and activation in recent years[25,26]. To explore Dai target in skin fibroblasts, we obtained the current bands by DARTS and in-gel digestion experiments, and determined that pyruvate kinase M2 (PKM2) is the most promising target of Dai through mass spectrometry. By molecular docking, we found that the docking score of Dai with PKM2 was − 5.94. Dai had hydrophobic interactions with amino acids VAL-58 C, GLU-59 C and LYS-230D. There is hydrogen bond interaction with amino acids VAL-58 C, GLU-59 C, LYS-62 C, GLN-227D (Fig. 7A). Then, immunohistochemistry results proved PKM2 was significantly increased after BLM induced, indicating that PKM2 could be enhanced in response to fibrosis (Fig. 7B). Besides, we conducted a CETSA experiment. Compared to the PBS group, Dai protects PKM2 from degradation with increasing temperature (Fig. 7C). To verify the biological role of PKM2 in DFs, we silenced PKM2 by siRNA-PKM2. We soon investigated the effects by knockdown PKM2 on fibrotic proteins, including Fn, Col-1 and P-Smad3. As expected, knockdown PKM2 decreased the expressions of Fn, Col-1 and P-Smad3, and it seemed no difference between Dai single group and Dai + si-PKM2 groups (Fig. 7D, E). Consistently, Dai could also attenuate PKM2 protein level in the keloid xenografts model (Figure S3). Taken together, these data demonstrated that Dai inhibited DFs activation through PKM2 by TGF-β1 induction.

Working model of Dai on skin fibrosis.

## Discussion

Keloid is a kind of skin fibrotic disease, which is recognized by over proliferation and over accumulation of the extracellular matrix of skin fibroblasts[17,18]. Although there is much research on the pathogenesis of keloids, the treatment of keloids still faces the drawback of a high rate of recurrence[19]. However, in our research, we found the potential effects of Dai on skin fibrosis. To begin with, results suggested that Dai alleviated the proliferation, migration, and activation of skin fibroblasts. Besides, results indicated that Dai ameliorated BLM-induced skin fibrosis and keloid xenograft[12,13].

Addressing the mechanism of action of Dai, we proved that Dai inhibited TGF-β/Smad signaling in a dose-dependent method and suppress TGF-β1-induced activation of skin fibroblasts. We further studied the target mechanism of Dai affecting TGF-β1 signaling pathway. Through mass spectrometry, we found that pyruvate kinase M2 (PKM2) may be a potential target of Dai. Molecular docking analysis and CETSA experiment verified the binding of Dai and PKM2. Next, we found silenced PKM2 significantly inhibited TGF-β1-induced phosphorylated Smad3 and fibrosis markers, with no significant difference between Dai treatment group and si-PKM2 + Dai treatment group. PKM2 is a key enzyme that catalyzes the last step of glycolysis, which could form

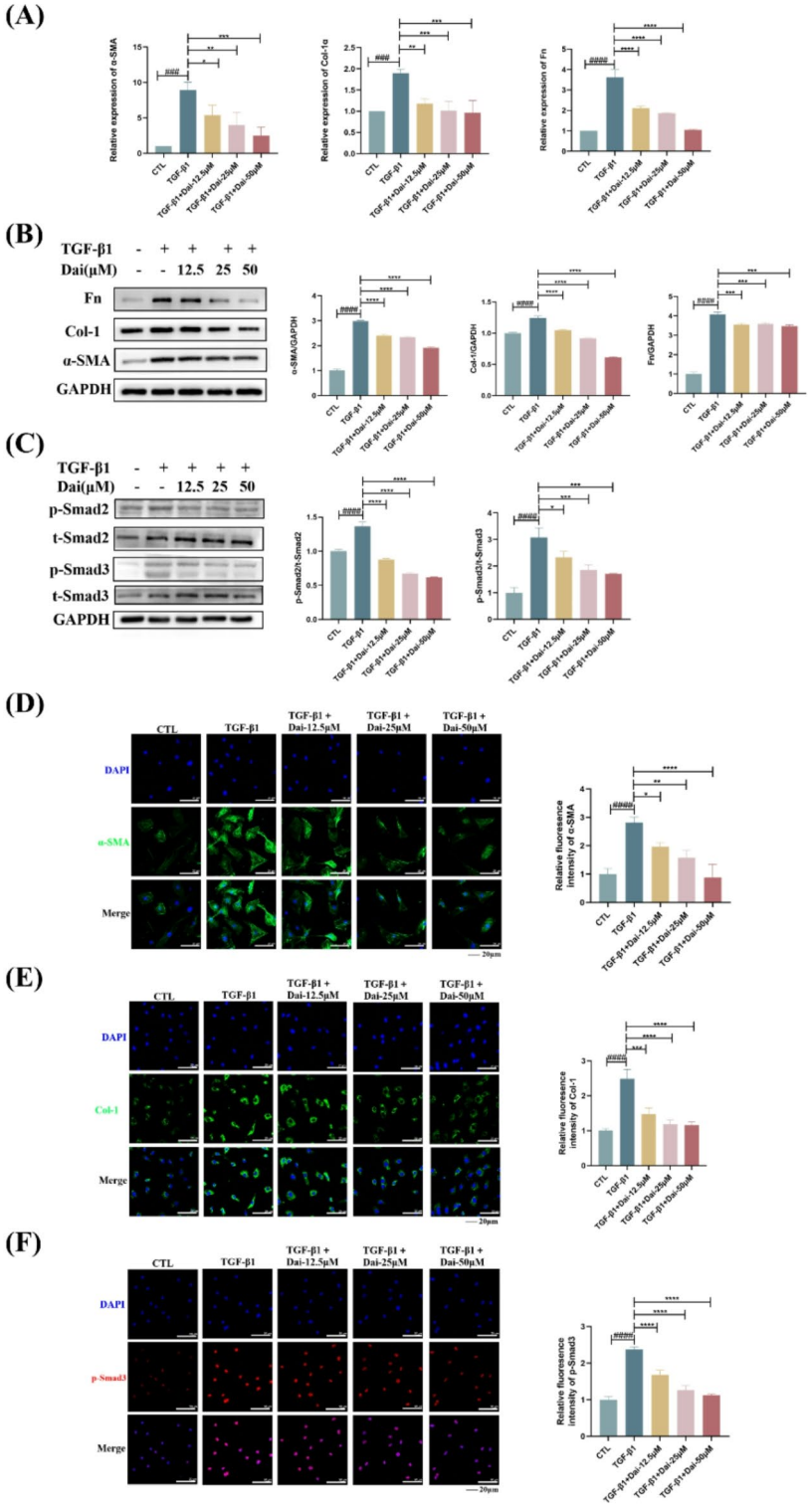


**Fig. 3**. Daidzein inhibits TGF-β1-induced activation of mouse primary dermal fibroblasts. (**A**) The mRNA levels of α-SMA, Col-1 and Fn in DFs ($n = 5$); (**B**) The protein levels of α-SMA, Col-1 and Fn in DFs ($n = 5$); (**C**) The protein levels of p-Smad2, t-Smad2, p-Smad3, t-Smad3 and GAPDH in DFs ($n = 5$); (D) Immunofluorescence representative images and quantitative results of α-SMA in DFs ($n = 5$) (40×, scale bar = 20 μm); (**E**) Immunofluorescence representative images and quantitative results of Col-1 in DFs ($n = 5$) (40×, scale bar = 20 μm); (**F**) Immunofluorescence representative images and quantitative results of p-Smad3 in DFs ($n = 5$) (40×, scale bar = 20 μm). The data are shown as Mean ± SD, one-way ANOVA with Tukey's post-hoc multiple comparison tests. ####, $p < 0.0001$ vs. CTL; *, $p < 0.05$, **, $p < 0.01$, ***, $p < 0.001$, ****, $p < 0.0001$ vs. TGF-β1. CTL, Control; Dai, Daidzein; DFs, Mouse primary dermal fibroblasts; Fn, Fibronectin; Col-1, Collagen-I.

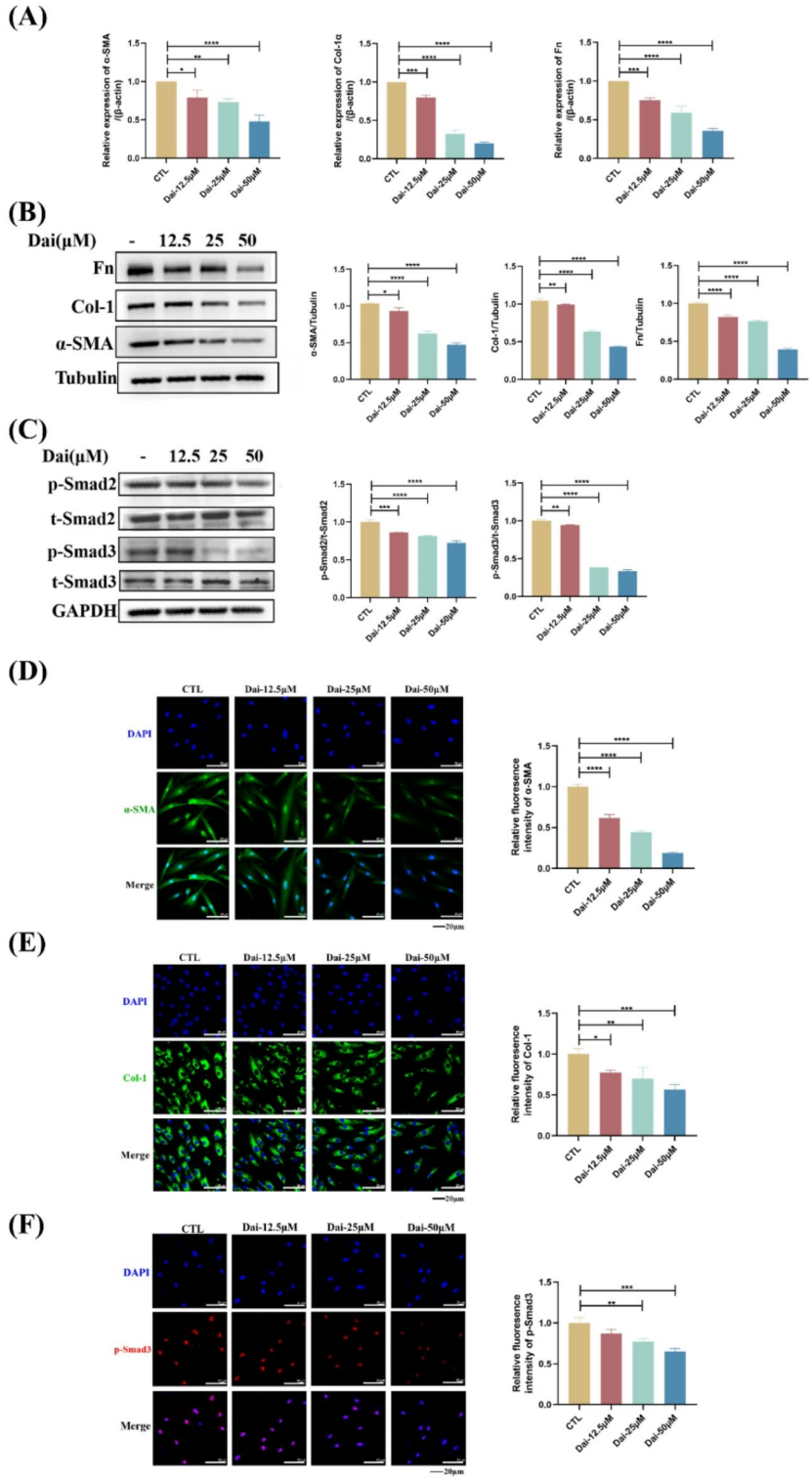


**Fig. 4**. Daidzein reduces fibrosis-associated expression of keloid pathogenesis in keloid fibroblasts. (**A**) The mRNA levels of α-SMA, Col-1 and Fn in KFs ($n = 5$); (**B**) The protein levels of α-SMA, Col-1, Fn and Tubulin in KFs ($n = 5$); (**C**) The protein levels of p-Smad2, t-Smad2, p-Smad3, t-Smad3 and GAPDH in KFs ($n = 5$); (**D**) Immunofluorescence representative images and quantitative results of α-SMA in KFs ($n = 5$) (40×, scale bar = 20 μm); (**E**) immunofluorescence representative images and quantitative results of Col-1 in KFs ($n = 5$) (40×, scale bar = 20 μm); (**F**) immunofluorescence representative images and quantitative results of p-Smad3 in KFs ($n = 5$) (40×, scale bar = 20 μm). The data are shown as Mean ± SD, one-way ANOVA with Tukey's post-hoc multiple comparison tests. *, $p < 0.05$, **, $p < 0.01$, ***, $p < 0.001$, ****, $p < 0.0001$ vs. CTL. CTL, Control; Dai, Daidzein; KFs, Keloid fibroblasts; Fn, Fibronectin; Col-1, Collagen-I.

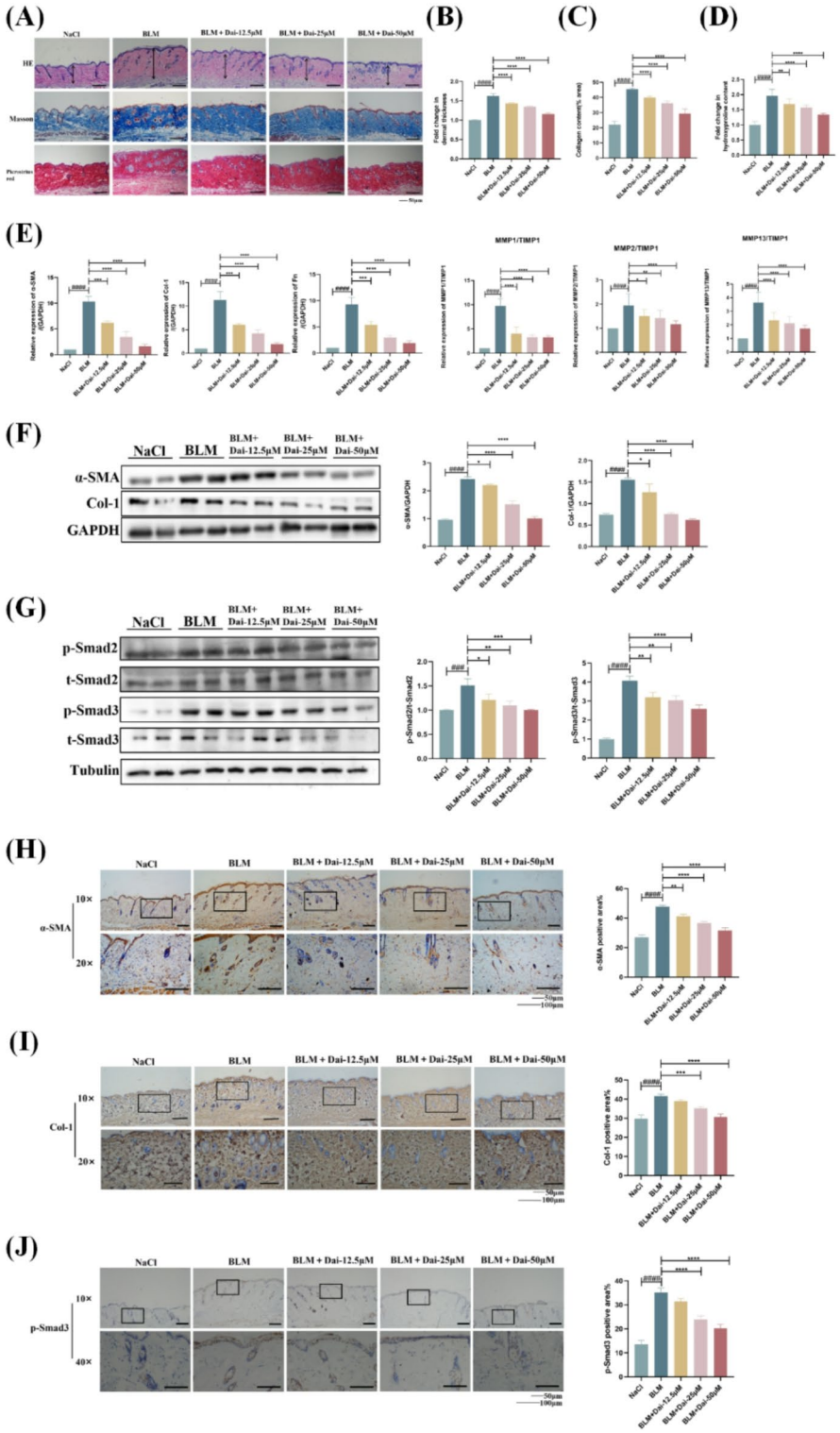


complex allosteric regulation to perform diverse biological functions. The tetramer form of PKM2 is a pyruvate kinase that regulates glycolysis[20], while the PKM2 dimer modulates gene transcription by translocation to the nucleus[21]. This property enables PKM2 to promote cell proliferation in both metabolic and non-metabolic ways, and therefore PKM2 is highly expressed in most cancers[22] and organ fibrotic diseases, including non-alcoholic steatohepatitis[23] and renal fibrosis[24]. Previous studies demonstrated that PKM2 modulated both typical and atypical TGFβ1 signaling pathways[25]. Besides, the studies of our research group found that PKM2 enhanced the progression of pulmonary fibrosis by directly interacting with Smad7 and enhancing TGFβ1 signaling[26]. Meanwhile, other research indicated that PKM2 was a specific target of Dai, and combined with previous studies in pulmonary fibrosis, PKM2 may be an important innovative target for skin fibrosis. However, little is known on the specific binging sites between Dai and PKM2. Indeed, further research still need to be done on the exact

◀**Fig. 5**. Daidzein alleviates BLM-induced skin fibrosis in mice and inhibits fibrogenic activation in vivo. (**A**) Representative skin sections stained with hematoxylin–eosin (H&E), Sirius red and Masson's trichrome staining of BLM-induced skin fibrosis ($n = 8$) (20×, scale bar = 50 μm); (**B**) Quantitative results of total dermal thickness ($n = 8$). The results were based on Hematoxylin–eosin (H&E) images; (**C**) Quantitative results of collagen content ($n = 8$). The results were based on Masson's trichrome and Sirius red images; (**D**) Hydroxyproline content of skin tissues in mice ($n = 8$); (**E**) The mRNA levels of α-SMA, Col-1, Fn, MMP-1, MMP-2 and MMP-13 in the lesional skin ($n = 8$); (**F**) The protein levels of α-SMA and Col-1 in the lesional skin ($n = 8$); (**G**) The protein levels of p-Smad2, t-Smad2, p-Smad3, t-Smad3 and Tubulin in the lesional skin ($n = 8$); (**H**) Immunohistochemical staining analysis of α-SMA in the lesional skin ($n = 8$) (10× and 20×, scale bar = 50 and 100 μm); (**I**) Immunohistochemical staining analysis of Col-1 in the lesional skin ($n = 8$) (10× and 20×, scale bar = 50 and 100 μm). (**J**) Immunohistochemical staining analysis of p-Smad3 in the lesional skin ($n = 8$) (10× and 40×, scale bar = 50 and 100 μm). The data are shown as Mean ± SD (one-way ANOVA with Tukey's post-hoc multiple comparison tests). ###, $p < 0.001$, ####, $p < 0.0001$ vs. NaCl; *, $p < 0.05$, **, $p < 0.01$, ***, $p < 0.001$, ****, $p < 0.0001$ vs. BLM. BLM, Bleomycin; Dai, Daidzein; Fn, Fibronectin; Col-1, Collagen-I.

effects of Dai with the structure and function of PKM2, evaluating whether Dai combinated other proteins associated with skin fibrosis as well.

In our study, we used a nude mouse keloid xenotransplantation model to mimic human scar disease. Studies have shown that keloid transplantation under the skin of nude mice has the ability of angiogenesis and continuous collagen synthesis, which can remain active for several weeks. Therefore, this model can be used to explored the result of drugs on clinical scar tissue[27]. However, this model is still not perfect, because nude mice showed limited transplantation rejection due to lack of functional T cells, but the mice still had congenital and humoral adaptive immune system functions, resulting in scar tissue gradually shrinking over time after transplantation into mice. There are limitations to model evaluation[28]. In addition, there is a PDX model that uses scar fibroblasts similar with tumor cells to be implanted under the skin of nude mice[29], which has the characteristics of continuous proliferation. We can try to further evaluate the efficacy of Dai by using this model. However, TGF-β/Smad signaling was considered as a protective signaling during skin aging process[30,31]. Although studies have shown that high doses of Dai could attenuate skin aging and enhance collagen-I synthesis by TGF-β/Smad signaling, which also indicated that Dai might be considered as possible anti-skin aging candidates in the future[32].

In conclusion, our research suggests that Dai may inhibit skin fibrosis in mouse models and keloid xenografts by targeting PKM2 to inhibit TGF-β1 signaling, which may provide more drug options for skin fibrosis (Fig. 8).

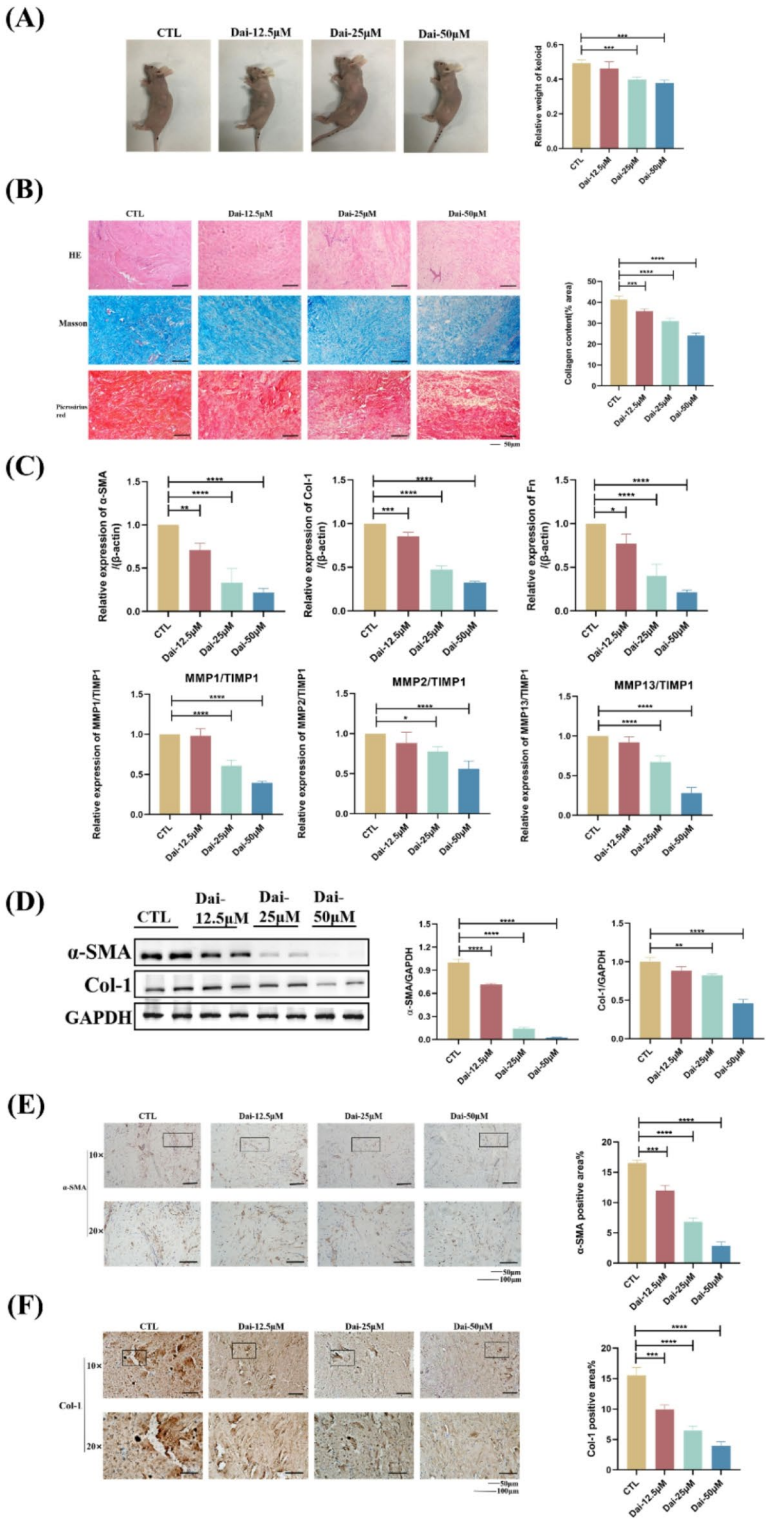


**Fig. 6**. Daidzein Reduces the Fibrogenic Activation of Xenografted Keloid Tissue. (**A**) Macrographic examination and weight of xenografted tissues on the back of nude BALB/c mice ($n = 4$). Weight of xenografted tissues were tested after intralesional injection of Dai; (**B**) Representative and quantitative results of xenografted tissues stained with hematoxylin-eosin (H&E), Sirius red and Masson's trichrome staining ($n = 4$) (20×, scale bar = 50 μm); (**C**) The mRNA levels of α-SMA, Col-1, Fn, MMP-1, MMP-2 and MMP-13 in the xenografted tissues ($n = 4$); (**D**) The protein levels of α-SMA and Col-1 in the xenografted tissues ($n = 4$); (**E**) Immunohistochemical staining analysis of α-SMA in the xenografted tissues ($n = 4$) (10× and 20×, scale bar = 50–100 μm); (**F**) Immunohistochemical staining analysis of Col-1 in the xenografted tissues ($n = 4$) (10× and 20×, scale bar = 50–100 μm). The data are shown as Mean ± SD (one-way ANOVA with Tukey's post-hoc multiple comparison tests). *, $p < 0.05$, **, $p < 0.01$, ***, $p < 0.001$, ****, $p < 0.0001$ vs. CTL. CTL, Control; Dai, Daidzein; Fn, Fibronectin; Col-1, Collagen-I.

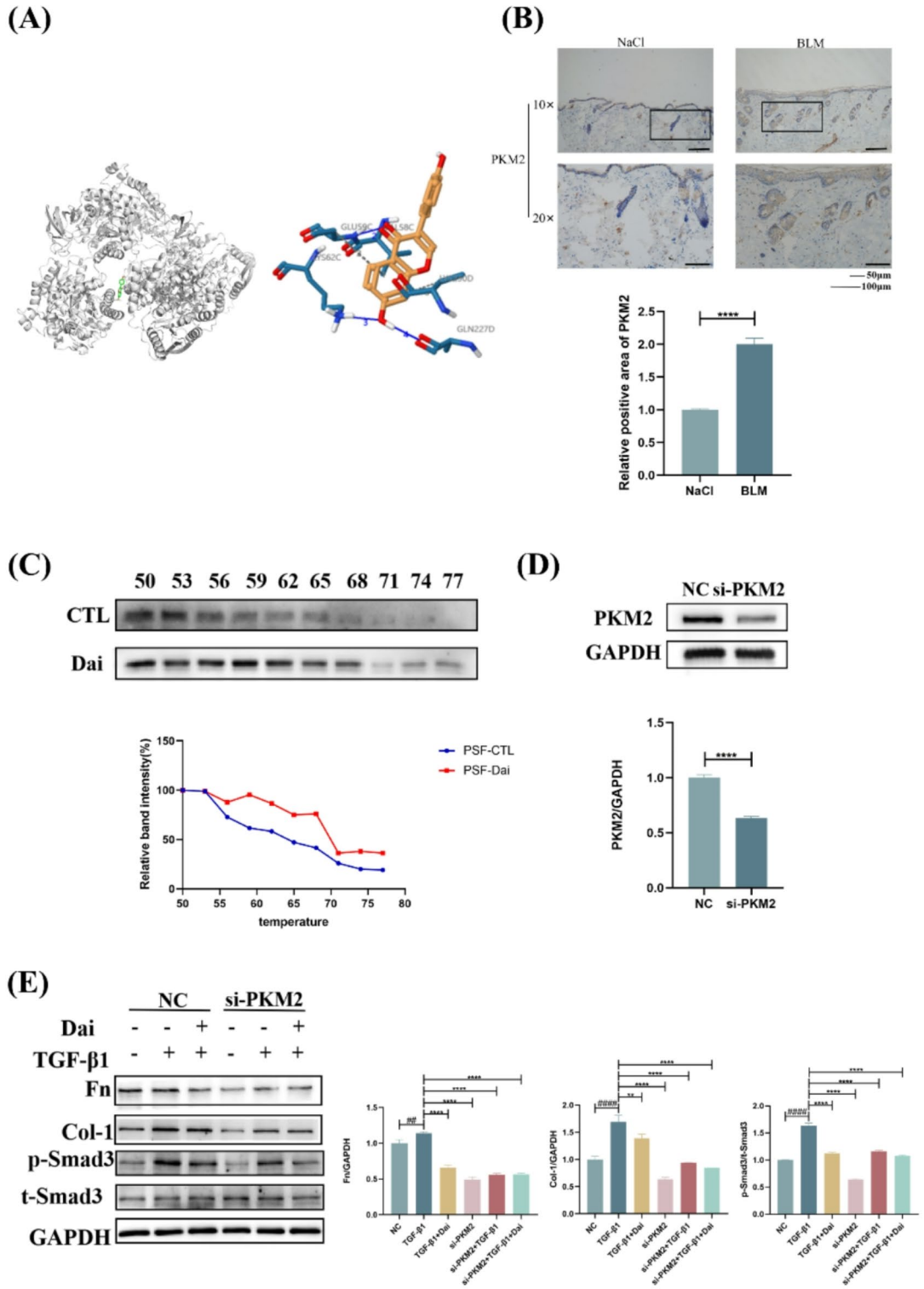


**Fig. 7**. Daidzein targets PKM2 to inhibit TGF-β1 signaling pathway. (**A**) Molecular docking showed binding domain of mouse PKM2 and Dai; (**B**) Immunohistochemical staining analysis of PKM2 in the lesional skin of BLM-induced skin fibrosis ($n = 4$) (10× or 20×, scale bar = 50–100 μm); (**C**) The interaction of PKM2 with Dai was measured by thermal displacement experiment in DFs ($n = 4$); (**D**) The knock-down efficiency of PKM2 in DFs ($n = 4$); (**E**) The protein levels of Fn, Col-1, p-Smad3, t-Smad3 and GAPDH with knockdown PKM2 in DFs ($n = 4$). The data are shown as Mean ± SD, one-way ANOVA with Tukey's post-hoc multiple comparison tests. ****, $p < 0.0001$ vs. NaCl / NC; ##, $p < 0.01$, ####, $p < 0.0001$ vs. CTL; *, $p < 0.01$, **, $p < 0.01$, ****, $p < 0.0001$ vs. TGF-β1. CTL, Control; Dai, Daidzein; DFs, Mouse primary dermal fibroblasts; Fn, Fibronectin; Col-1, Collagen-I.

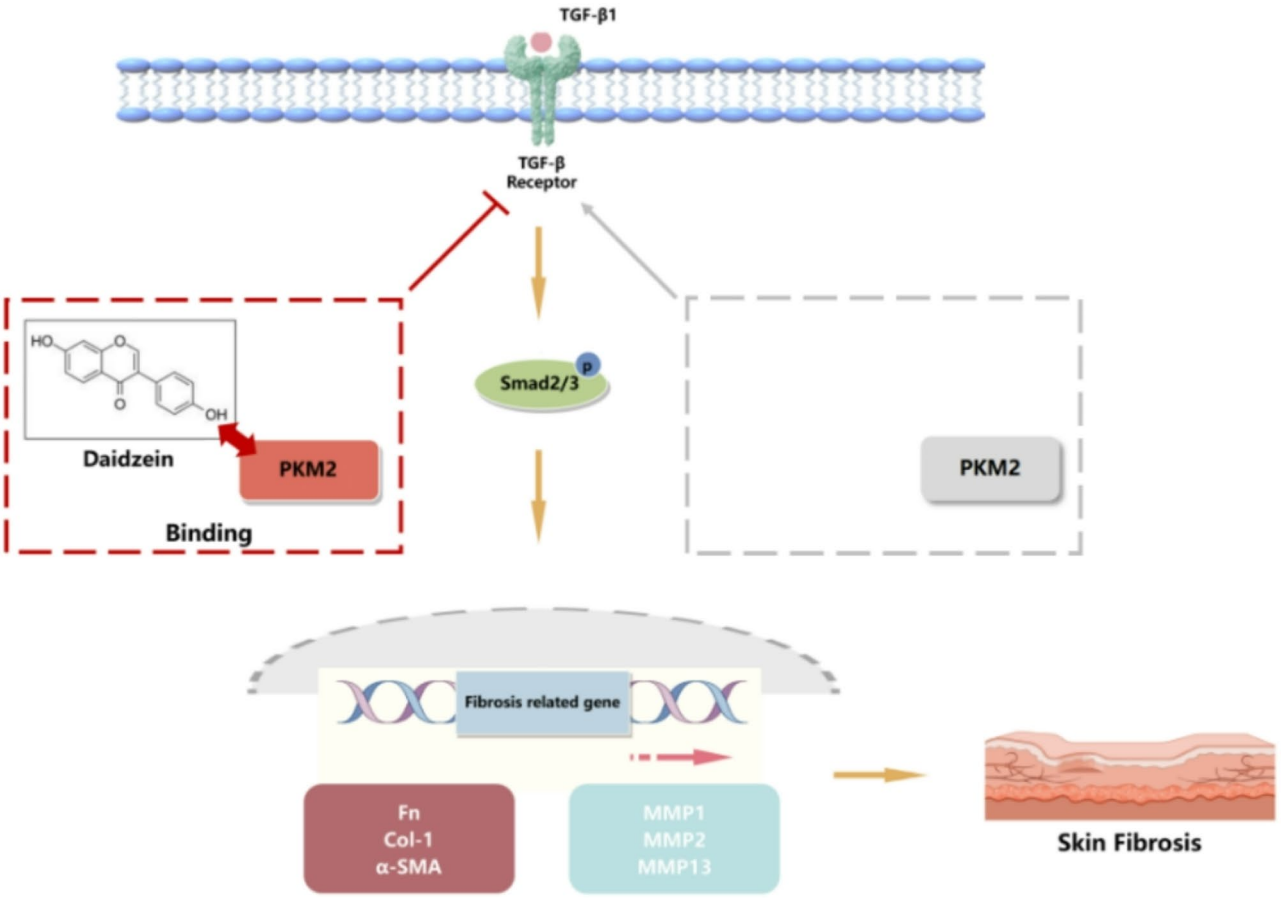


**Fig. 8**. Working model of Dai on skin fibrosis.

## Data availability

The data that support the findings of this study are available in the Materials and Methods, Results, and/or Supplemental Material of this article.

Received: 29 September 2024; Accepted: 4 March 2025
Published online: 13 March 2025

## References

1. Maria, A. T. J. B. C. et al. De La fibrogenèse à La fibrose: mécanismes physiopathologiques et présentations cliniques [From fibrogenesis towards fibrosis: Pathophysiological mechanisms and clinical presentations]. *Rev. Med. Interne*. **41**, 325–329 (2020).
2. Pedroza, M. et al. Role of STAT3 in skin fibrosis and transforming growth factor beta signalling. *Rheumatology* **57**, 1838–1850 (2018).
3. Bran & Keloids Current concepts of pathogenesis (Review). *Int. J. Mol. Med.* **24** (2009).
4. Wang, Q. et al. Altered glucose metabolism and cell function in keloid fibroblasts under hypoxia. *Redox Biol.* **38** (2021).
5. Li, Y. et al. The polygenic map of keloid fibroblasts reveals Fibrosis-Associated gene alterations in inflammation and immune responses. *Front. Immunol.* **12** (2022).
6. Li, X. et al. Pinocembrin ameliorates skin fibrosis via inhibiting TGF-β1 signaling pathway. *Biomolecules* **11** (2021).
7. Cui, J., Shan Jin, Jin, C. & Jin, Z. Syndecan-1 regulates extracellular matrix expression in keloid fibroblasts via TGF-β1/Smad and MAPK signaling pathways. *Life Sci.* **254** (2020).
8. Jiang, Z. et al. Growth differentiation Factor-9 promotes fibroblast proliferation and migration in keloids through the Smad2/3 pathway. *Cell. Physiol. Biochem.* **40**, 207–218 (2016).
9. Andrews, J. P. et al. The paradigm of skin fibrosis — Pathomechanisms and treatment. *Matrix Biol.* **51**, 37–46 (2016).
10. Cayetano-Salazar, L. et al. Natural isoflavonoids in invasive cancer therapy: from bench to bedside. *Phytother Res.* **35**, 4092–4110 (2021).
11. Li, H. et al. Daidzein alleviates doxorubicin-induced heart failure via the SIRT3/FOXO3a signaling pathway. *Food Funct.* **13**, 9576–9588 (2022).
12. Shu, J. et al. Daidzein suppresses TGF-β1-induced cardiac fibroblast activation via the TGF-β1/SMAD2/3 signaling pathway. *Eur. J. Pharmacol.* 919. (2022).
13. Soumyakrishnan, S., Divya, T., Kalayarasan, S., Sriram, N. & Sudhandiran, G. Daidzein exhibits anti-fibrotic effect by reducing the expressions of proteinase activated receptor 2 and TGFβ1/smad mediated inflammation and apoptosis in Bleomycin-induced experimental pulmonary fibrosis. *Biochimie* **103**, 23–26 (2014).
14. Zhou, B. et al. Nintedanib inhibits keloid fibroblast functions by blocking the phosphorylation of multiple kinases and enhancing receptor internalization. *Acta Pharmacol. Sin.* **41**, 1234–1245 (2020).

15. Li, X. et al. Targeting FSTL1 for multiple fibrotic and systemic autoimmune diseases. *Mol. Ther.* **29**, 347–364 (2021).
16. Darmawan, C. C. et al. Adiponectin-Based peptide (ADP355) inhibits transforming growth Factor-β1-Induced fibrosis in keloids. *Int. J. Mol. Sci.* **21**. (2020).
17. Eming, S. A., Martin, P. & Tomic-Canic, M. Wound repair and regeneration: mechanisms, signaling, and translation. *Sci. Transl. Med.* **6**. (2014).
18. MD MLE. Update on management of keloid and hypertrophic scars: A systemic review. *J. Cosmet. Dermatol.* **20**, 2729–2738 (2021).
19. Zhang, T. et al. Current potential therapeutic strategies targeting the TGF-β/Smad signaling pathway to attenuate keloid and hypertrophic Scar formation. *Biomed. Pharmacother.* 129 (2020).
20. Witney, T. H. et al. PET imaging of tumor Glycolysis downstream of hexokinase through noninvasive measurement of pyruvate kinase M2. *Sci. Transl Med.* 7 (2015).
21. Yang, W. et al. Nuclear PKM2 regulates β-catenin transactivation upon EGFR activation. *Nature* **480**, 118–122 (2011).
22. Lin, Y. et al. Knockdown of PKM2 enhances radiosensitivity of cervical cancer cells. *Cancer Cell Int.* 19. (2019).
23. Xu, F. et al. Annexin A5 regulates hepatic macrophage polarization via directly targeting PKM2 and ameliorates NASH. *Redox Biol.* 36. (2020).
24. Liu, H., Takagaki, Y., Kumagai, A., Kanasaki, K. & Koya, D. The PKM2 activator TEPP-46 suppresses kidney fibrosis via Inhibition of the EMT program and aberrant Glycolysis associated with suppression of HIF-1α accumulation. *J. Diabetes Invest.* **12**, 697–709 (2020).
25. Zhang, X. et al. PKM2 promotes angiotensin-II-induced cardiac remodelling by activating TGF-β/Smad2/3 and Jak2/Stat3 pathways through oxidative stress. *J. Cell. Mol. Med.* **25**, 10711–10723 (2021).
26. Gao, S. L. X. et al. PKM2 promotes pulmonary fibrosis by stabilizing TGF-β1 receptor I and enhancing TGF-β1 signaling. *Sci. Adv.* 8. (2022).
27. Marttala, J., Andrews, J. P., Rosenbloom, J. & Uitto, J. Keloids: animal models and pathologic equivalents to study tissue fibrosis. *Matrix Biol.* **51**, 47–54 (2016).
28. Seo, B. F., Lee, J. Y. & Jung, S-N. Models of abnormal scarring. *BioMed Res. Int.* 1–8. (2013).
29. Choi, M-H., Kim, J., Ha, J. H. & Park, J-U. A selective small-molecule inhibitor of c-Met suppresses keloid fibroblast growth in vitro and in a mouse model. *Sci. Rep.* **11** (2021).
30. Fisher, G. J. et al. Reduction of fibroblast size/mechanical force down-regulates TGF-β type II receptor: implications for human skin aging. *Aging Cell.* **15**, 67–76 (2016).
31. Xu, D., Li, C. & Zhao, M. Attenuation of UV-induced skin Photoaging in rats by walnut protein hydrolysates is linked to the modulation of MAPK/AP-1 and TGF-β/Smad signaling pathways. *Food Funct.* **13**, 609–623 (2022).
32. Zhao, D., Shi, Y., Dang, Y., Zhai, Y. & Ye, X. Daidzein stimulates collagen synthesis by activating the TGF-β/smad signal pathway. *Australas J. Dermatol.* ;**56** (2015).


## Author contributions

Xiaowei Guo: Conceptualization, Data curation, Investigation, Software, Writing-original draft, Writing-review & editing; Wenqi Li: Conceptualization, Data curation, Investigation, Software, Writing-original draft, Writing-review & editing; Wei Ma: Conceptualization, Data curation, Funding acquisition, Resources, Writing-original draft, Writing-review & editing; Yuming Liu: Formal analysis, Investigation, Methodology; Zhigang Liu: Formal analysis, Investigation, Methodology; Ran Jiao: Investigation, Methodology; Zhongyi Yang: Investigation, Methodology; Tiantian Zhang: Investigation, Methodology; Hongliang Wu: Funding acquisition, Project administration, Resources, Software; Xiaoyu Ai: Funding acquisition, Project administration, Resources, Software; Xiaoting Gu: Funding acquisition, Project administration, Resources, Software; Wendi Wang: Project administration, Resources, Software; Honggang Zhou: Project administration, Supervision, Validation, Visualization, Writing-review & editing; Xiaohe Li: Supervision, Validation, Visualization, Writing-review & editing; Cheng Yang: Supervision, Validation, Visualization, Writing-review & editing. All authors have read and agreed to the published version of the manuscript.

## Funding

This work was supported by Tianjin Health Science and technology project [No. TJWJ2021YJ001], The Natural Science Foundation of Tianjin, China [Grant 22JCQNJC01610 and Grant 22JCQNJC00510], CAMS Innovation Fund for Medical Sciences (CIFMS) [Grant 2021-I2M-C&T-B-049].

## Declarations

## Competing interests

The authors declare no competing interests.

## Additional information

**Supplementary Information** The online version contains supplementary material available at https://doi.org/10.1038/s41598-025-93007-3.

**Correspondence** and requests for materials should be addressed to H.Z., X.L. or C.Y.